CHEMISTRY
A EUROPEAN JOURNAL

DOI: 10.1002/chem.200800096

On the Mechanism of the Thermal Retrocycloaddition of Pyrrolidinofullerenes (Retro-Prato Reaction)

Salvatore Filippone,[a] Marta Izquierdo Barroso,[a] Ángel Martín-Domenech,[a] Sílvia Osuna,[b] Miquel Solà,*[b] and Nazario Martín*[a]

Abstract: In contrast to *N*-methyl or N-unsubstituted pyrrolidinofullerenes, which efficiently undergo the retrocycloaddition reaction to quantitatively afford pristine fullerene, *N*-benzoyl derivatives do not give this reaction under the same experimental conditions. To unravel the mechanism of the retrocycloaddition process, trapping experiments of the in-situ thermally generated azomethine ylides, with an efficient dipolarophile were conducted. These experiments afforded the respective cycloadducts as an *endo*/*exo* isomeric mixture. Theoretical calculations carried out at the DFT level and by using the two-layered ONIOM (our own *n*-layered integrated molecular orbital and molecular mechanics) approach underpin the experimental findings and predict that the presence of the dienophile is not a basic requirement for the azomethine ylide to be able to leave the fullerene surface under thermal conditions. Once the 1,3-dipole is generated in the reaction medium, it is efficiently trapped by the dipolarophile (maleic anhydride or *N*-phenylmaleimide). However, for N-unsubstituted pyrrolidinofullerenes, the participation of the dipolarophile in assisting the 1,3-dipole to leave the fullerene surface throughout the whole reaction pathway is also a plausible mechanism that cannot be ruled out.

Keywords: density functional calculations · fullerenes · nanostructures · reaction mechanisms · retrocycloaddition

Introduction

Since the discovery of fullerenes by Sir H. W. Kroto, R. F. Curl, and the late R. E. Smalley in 1985,[1] and the closely related carbon nanotubes by Iijima in 1991,[2] other new forms of carbon allotropes, namely, endohedral and higher fullerenes, nanohorns, nanoonions, and graphenes have been reported.[3] Much effort is currently dedicated to understanding the chemical reactivity of these fascinating three-dimensional all-carbon nanostructures in order to prepare soluble and easy-to-handle materials in the search for new properties for practical applications.[4] However, despite the interest in new carbon allotropes, the chemistry of fullerenes has not settled down and the synthesis of intriguing new structures with unexpected properties is still possible on the fullerene sphere.[5] In fact, the convex surface of fullerenes formed by the highly reactive double bonds that protrude from the spherical surface is a unique location for testing a wide variety of challenging new reactions. Moreover, the reactivity of fullerenes is an excellent benchmark for understanding the chemical behaviour of the above-mentioned less-accessible and still scarcely known new nanoforms of carbon.

During recent years, we have studied new reactions on the fullerene sphere, by using 1,6-fullerenynes as a versatile building block, such as the well-known [2+2+1] Pauson–Khand reaction,[6] which despite its usefulness for the creation of carbocyclic rings has been almost neglected in materials science; the thermally induced [2+2] cyclization, which forms unprecedented cyclobutene-fused carbocycles without involving the presence of any catalyst[7] and the thermal intramolecular ene reaction which leads to new and less-known fullerenes decorated with the allene functionality.[8]

---

[a] Dr. S. Filippone, M. I. Barroso, Dr. Á. Martín-Domenech,
Prof. Dr. N. Martín
Departamento de Química Orgánica
Facultad de Ciencias Químicas, Universidad Complutense de Madrid
Ciudad Universitaria s/n 28040 Madrid (Spain)
Fax: (+34) 913-944-103
E-mail: nazmar@quim.ucm.es

[b] S. Osuna, Prof. Dr. M. Solà
Institut de Química Computacional i Departament de Química
Universitat de Girona, Campus Montilivi
17071 Girona, Catalonia (Spain)
Fax: (+34) 972-418-356
E-mail: miquel.sola@udg.edu

Supporting information for this article is available on the WWW under http://www.chemeurj.org/ or from the author.

Furthermore, in a preliminary communication we have recently reported the highly efficient thermal retrocycloaddition reaction of the well-known pyrrolidinofullerenes (pyrrolidino[3,4:1,2,60]fullerenes).[9] These modified fullerenes are among the most useful and studied fullerene derivatives due to their easy synthetic preparation.[10] In contrast to other fullerene derivatives, such as Diels–Alder cycloadducts[11] or Bingel's methanofullerenes,[12] which undergo the corresponding retrocycloaddition reactions, pyrrolidinofullerenes have been considered to be very stable cycloadducts and, therefore, this functionalization has been chosen as a suitable procedure for the preparation of a wide variety of fullerene derivatives of interest in biomedicine and in materials science.[13]

In this paper, we report on new experimental and theoretical studies carried out on the retro-Prato reaction to determine a plausible mechanism by which these modified fullerenes afford pristine fullerenes by thermal treatment in the presence of a large excess of an efficient dipolarophile. Whereas trapping experiments were carried out to confirm the presence of the azomethine ylide as an intermediate 1,3-dipole in the retrocyclization process, theoretical calculations at the DFT level by using the two-layered ONIOM (ONIOM = our own *n*-layered integrated molecular orbital and molecular mechanics) approach were performed to underpin the experimental findings.

Results and Discussion

Synthesis and trapping experiments: In a preliminary communication we have shown that the retrocycloaddition of *N*-methylpyrrolidinofullerenes (*N*-methyl pyrrolidino[3,4:1,2,60]fullerenes) occurs quantitatively by simply heating the starting materials at reflux in *o*-dicholorobenzene (*o*-DCB) for 24 h in the presence of an excess (30 equiv) of a good dipolarophile, such as maleic anhydride or *N*-phenylphthalimide. This is a very general procedure with a broad scope of applicability.[9] In fact, the initial brown solution of the *N*-methylpyrrolidinofullerenes turns the magenta color typical of pristine [60]fullerene solutions after the retrocyclization process. Furthermore, the reaction has also been shown to be highly efficient with *N*-methylpyrrolidino[3,4:1,2,70]fullerenes and, even more important, it allows the transformation of the undesired bis- and tris-cycloadducts—formed as byproducts in the synthesis of pyrrolidinofullerenes—into the respective monoadducts, thus improving significantly the yields of the Prato monoadducts.

In a general sense, the formation of *N*-methylpyrrolidinofullerenes and their subsequent quantitative thermal retrocyclization results in a new protection–deprotection protocol that has already been successfully used in the separation of the two constitutional isomers (I_h and D_{5h}) of trimetallic nitride endohedral metallofullerene $Sc_3N@C_{80}$.[9] We have also reported the efficient removal of pyrrolidine rings from fullerenes by controlled-potential electrochemical oxidation, to efficiently afford pristine fullerene.[14] To unravel the mechanism of this novel and versatile retrocycloaddition reaction, we have carried out new reactions on pyrrolidinofullerenes, in which the methyl (alkyl) group on the nitrogen atom has been substituted by a hydrogen atom (free pyrrolidine) or by a benzoyl group to determine the scope of the reaction. To this end, we have also carried out trapping experiments of the expected azomethine ylide, generated in situ as an intermediate 1,3-dipole, by means of the excess of dipolarophile (*N*-phenylmaleimide) present in the reaction medium (Scheme 1).

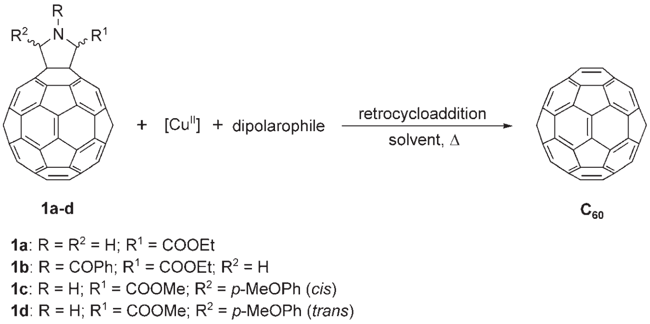

Scheme 1. Thermal retrocyclization of pyrrolidinofullerenes **1a–d**.

Thus, new pyrrolidinofullerenes (**1a–d**) were prepared by following the standard protocol from glycine and the respective reagents by following Prato's procedure (see the Experimental Section in the Supporting Information). Compound **1b** was prepared from **1a** by treatment with benzoyl chloride, which allowed the N-benzoylation of the pyrrolidine nitrogen atom. The thermal retrocycloaddition experiments carried out with compounds **1a–d** are shown in Table 1.

Table 1. Experimental conditions used in the retrocycloaddition reaction.

Entry	Compound	Dipolarophile (30 equiv)	Catalyst	Solvent	*t* [h]	Yield [%]
1	**1a**	–	–	*o*-DCB	24	90.0
2	**1a**	maleic anhydride	–	*o*-DCB	24	95.0
3	**1a**	maleic anhydride	$CuTf_2$[a]	*o*-DCB	24	99.0
4	**1a**	*N*-phenyl maleidimide	$CuTf_2$[a]	*o*-DCB	24	99.0
5	**1b**	–	–	*o*-DCB	24	0.0
6	**1b**	maleic anhydride	–	*o*-DCB	24	0.0
7	**1b**	maleic anhydride	$CuTf_2$[a]	*o*-DCB	24	27.3
8	**1c**	maleic anhydride	–	toluene	18	quant.
9	**1c**	maleic anhydride	$CuTf_2$[a]	toluene	18	quant.
10	**1d**	maleic anhydride	–	toluene	18	quant.
11	**1d**	maleic anhydride	$CuTf_2$[a]	toluene	18	quant.

[a] Copper(II) triflate (1 equiv).

A first and significant observation to unravel the mechanism of the retrocycloaddition process in pyrrolidinofullerenes is that compound **1a** can undergo the thermal retrocyclization in the absence of the dipolarophile to afford C_{60} in 90 % yield (entry 1). The presence of the dipolarophile increases the efficiency of the process (95 %, entry 2), and the addition of copper triflate as a catalyst results in the formation of [60]fullerene in a quantitative yield.

Interestingly, whereas compounds **1a**,**c**,**d** efficiently undergo the retrocyclization process to quantitatively form pristine [60]fullerene (entries 1–4, 8–11), *N*-benzoyl derivative **1b** did not to any extent afford pristine C_{60} (entries 5,6). This behaviour is in contrast to that previously observed for *N*-methylpyrrolidinofullerenes which quantitatively lead to [60]fullerene,[9] and confirms the importance of the nitrogen lone pair in the retrocycloaddition process. Compound **1b** affords C_{60} in the presence of a copper catalyst (Entry 7), although in a very poor yield; this could be accounted for by previous decomposition of the *N*-benzoyl derivative. Because the benzoylation of the pyrrolidine ring is a reversible process, we can take advantage of this discovery and use it to selectively preserve a benzoylated pyrrolidine in the presence of other unsubstituted or *N*-methyl substituted pyrrolidine rings under the conditions used for the retrocycloaddition process.

The presence of an aryl substituent on C-5 of the pyrrolidine ring with an ester group on C-2 results in an easier retrocyclization process that now takes place in refluxing toluene over a shorter period of time (entries 8–11). These results clearly indicate that the simultaneous presence of substituents, such as ester and aryl groups, which stabilize the in-situ-generated azomethine ylide, favor the retrocycloaddition process, which now occurs easily under the standard experimental conditions and, therefore, no additional catalyst is needed.

To prove that the azomethine ylide is formed as an intermediate in the retrocycloaddition process, we carried out trapping experiments by using *N*-phenylmaleimide (NPM)—instead of the less stable maleic anhydride—as the dipolarophile, under the same experimental conditions. Thus, compound **2** was refluxed in *o*-DCB in the presence of an excess of NPM (10 equivalents). In addition to C_{60} (70 %), the cycloadduct (**3**), which resulted from 1,3-dipolar cyloaddition of the in situ generated azomethine ylide to NPM, was obtained in 19 % yield as a 66:33 *endo*/*exo* mixture (Scheme 2). The structure of compound **3** was determined by spectroscopic techniques and confirmed by an alternative synthesis from the in-situ-generated azomethine ylide and NPM as previously reported in the literature.[15]

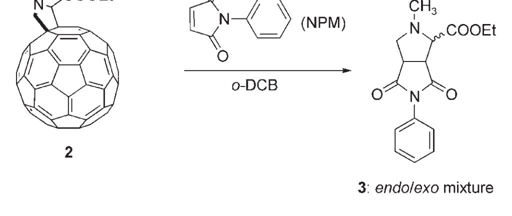

Scheme 2. Trapping experiment by using NPM as the dipolarophile.

The above trapping experiment clearly confirms that the reaction mechanism of the retrocycloaddition process occurs by thermal removal of the azomethine ylide as a 1,3-dipole, which is generated in situ under the experimental conditions used and the stability of which is highly dependent on the nature of the substituents. Whether the dipolarophile (NPM) is involved in the mechanism by assisting the 1,3-dipole to leave in a concerted way or whether it acts in a further step is an open question that we have addressed by means of theoretical calculations (see below).

Theoretical calculations: As discussed above, under thermal treatment and in the presence of an excess of a dipolarophile, such as maleic anhydride or NPM, pyrrolidino[3,4:1,2,60]fullerenes can efficiently revert to [60]fullerenes and azomethine ylides. This reaction is favored by the presence of substituents that stabilize the leaving 1,3-dipole. The effect of the substituent and the dipolarophile may be thermodynamic in the sense that they help to stabilize the final separated products and/or kinetic if the energy barrier that needs to be surmounted is reduced. To analyze whether the effects of the substituent and the dipolarophile in the retro-Prato reaction are thermodynamic and/or kinetic in nature, we have carried out a theoretical analysis of the reaction mechanisms depicted in Schemes 3 and 4 for compounds **4a** ($R^1 = H$) and **4b** ($R^1 = COOCH_3$). We have located every intermediate (int) and transition state (TS) involved in the four reactions studied (optimized *xyz* coordinates of all species are given as Supporting Information).

Retrocycloaddition without a dipolarophile: Our analysis starts with retrocycloaddition in the absence of any dipolarophile for the unsubstituted case. Theoretical studies of the 1,3-dipolar cycloadditions of different 1,3-dipoles (alkyl azides,[16,17] ozone,[18] and 3-phenylphthalazinium-1-olate[19]) to the [6,5]- and [6,6]-bonds of C_{60} have been made by several authors. In all cases, the cycloadditions that take place on [6,6]-bonds have been found to be clearly exothermic giving rise to stable adducts on crossing a relatively small energy barrier, whereas those that occur on the [6,5]-bonds are less favorable. In agreement with these previous results, we found that the retro-1,3-dipolar cycloaddition reaction starting from the [6,6]-adduct **4a** was endothermic by 53.1 kcal mol^{-1} and had a high energy barrier of 45.4 kcal mol^{-1}. The Gibbs free energy of the reaction and energy barrier are somewhat smaller, 33.9 and 39.2 kcal mol^{-1} as expected from the fact that there is an increase in the entropy along the reaction coordinate. The structure of the TS is given in Figure 1.[20] The dark grey atoms in Figure 1 constitute the small system treated at a high level of theory within the ONIOM approach for all species analyzed in this work. As can be seen in Figure 1, the reaction occurs through a concerted and almost synchronic TS with a distance of about 2.71 Å between the two C atoms of the C−C bonds that are

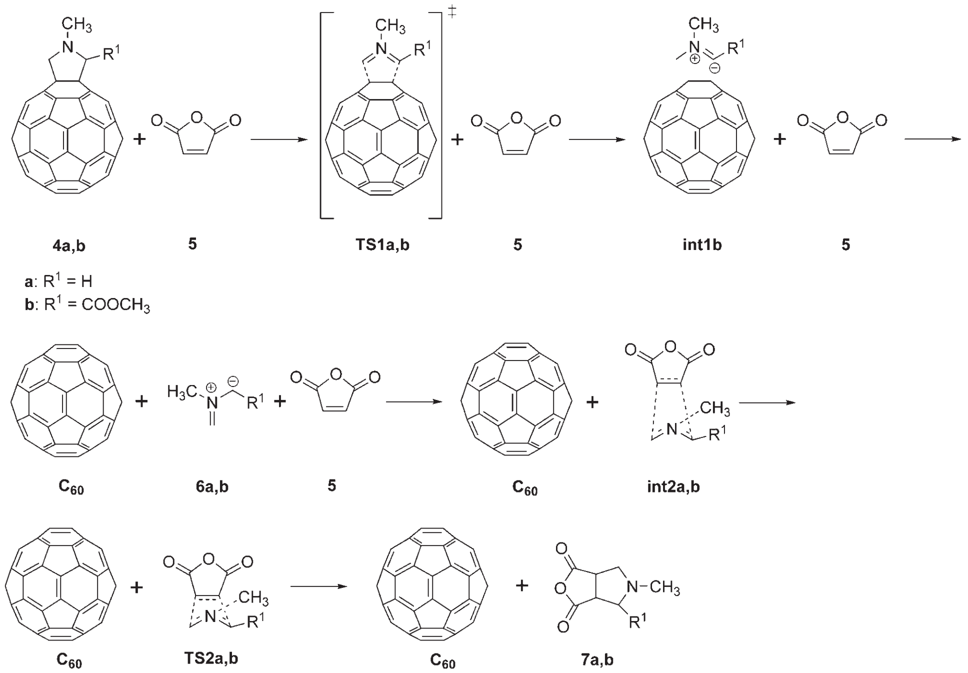

Scheme 3. Schematic representation of the different stationary points found along the pathway of the retrocycloaddition reaction assisted by the dipolarophile only at the last stage of the reaction.

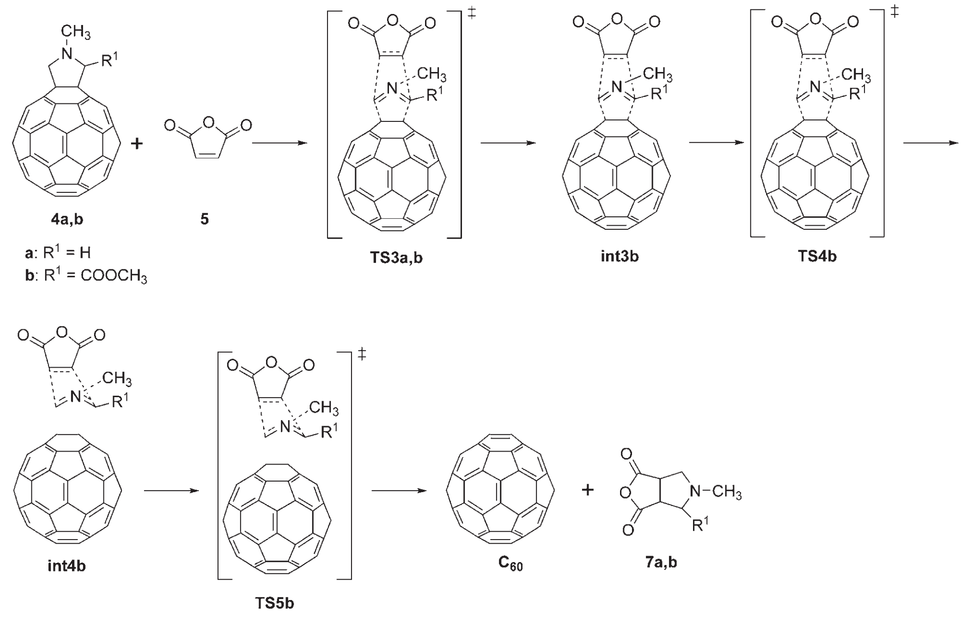

Scheme 4. Schematic representation of the different stationary points found along the pathway of the retrocycloaddition reaction assisted by maleic anhydride.

being broken. It is worth noting that in all cases we have analyzed both *exo* and *endo* approaches and we report here only the most stable TS.

Since the energy of the products (C_{60}+**6a**+**5**) is higher than that of the TS (see the whole energy profile in Figure 2), a minimum structure should be found between these two stationary points. To find such a minimum, a full optimization starting from the transition state was done by slightly shifting the geometry of the transition state whilst following the transition vector in the direction of the products. Unfortunately, all attempts to find this minimum structure failed and the optimization process yielded, in all cases, the original reactant **4a**. We think that this behavior indicates the existence of a very shallow minimum very close to the TS. This is in agreement with the fact that the region around the TS is extremely flat. Indeed, the imaginary frequency corresponding to the transition vector is only 33.8i cm^{-1}, which is also in accordance with the fact that any optimization we have carried out by starting from any structure close to the final products (for instance by starting from C–C bond distances of 4 Å) reverts to the initial reactant. The height for the activation barrier together with the endothermic nature of the process prevents the retrocycloaddition from occurring, as found experimentally.[9]

The second reaction mechanism that we have analyzed is the retrocycloaddition for the substituted species **4b** (R^1= $COOCH_3$, Scheme 3) to examine the effect of the substituent in the retro-Prato cycloaddition without a dipolarophile (**4b**→**C$_{60}$**+**6b**). As can be seen from the values in Figure 3, the substituent favors the retrocycloaddition by reducing the energy barrier by about 10 $kcal\,mol^{-1}$ and the reaction energy by about 15 $kcal\,mol^{-1}$. The reduction in the Gibbs free energies when going from an unsubstituted to a substituted reactant is somewhat lower (about 2 $kcal\,mol^{-1}$). The origin of the stabilization (10–15 $kcal\,mol^{-1}$ along the reaction coordinate) has to be attributed to the electron-withdrawing character from both inductive and resonance effects of the $COOCH_3$ substituent[21] that stabilizes the azomethine ylide formed. This effect is especially important at the end of the reaction, and for this reason the reaction energy is lowered more than the energy barrier. To illustrate this fact in more

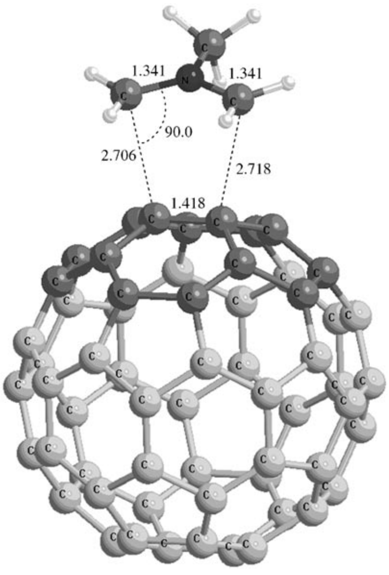

Figure 1. Optimized structure (ONIOM2(UB3LYP/6-31G(d):SVWN/STO-3G)) for **TS1a** with the most relevant bond lengths [Å] and angles [°]. H atoms and dark-grey atoms constitute the small system treated at a high level in the ONIOM approach.

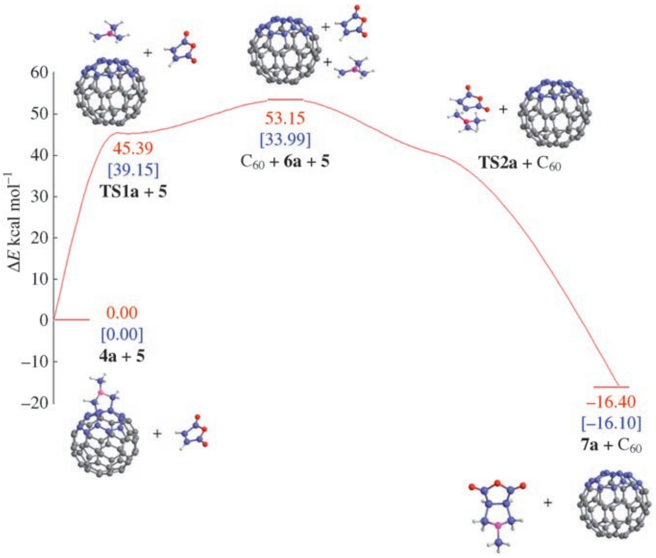

Figure 2. ONIOM2(UB3LYP/6-31G(d):SVWN/STO-3G) reaction energy profile (Gibbs free energies in square brackets) for the retrocycloaddition reaction of the unsubstituted system without a dipolarophile, except for the last step of the reaction.

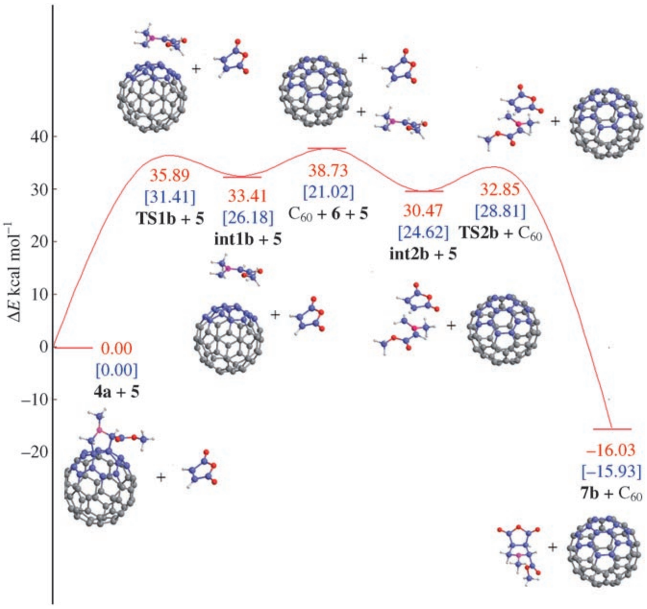

Figure 3. ONIOM2(UB3LYP/6-31G(d):SVWN/STO-3G) reaction energy profile (Gibbs free energies in square brackets) for the retrocycloaddition reaction of the substituted system ($R^1=COOCH_3$) without a dipolarophile, except for the last step of the reaction.

detail, we have computed the energy barriers for two more substituents: $R^1=OH$ and $R^1=CN$. For the former, the reaction energy increases by 5.1 kcal mol^{-1} relative to the unsubstituted case (53.1 kcal mol^{-1}). This is in agreement with OH being an electron-donating substituent.[21] On the other hand, for $R^1=CN$, another electron-withdrawing substituent,[21] the reaction energy decreases by 15.3 kcal mol^{-1}, not far from the 14.4 kcal mol^{-1} reduction observed for $R^1=COOCH_3$. Thus, there is a clear electronic effect of the pyrrolidine substituent: electron-withdrawing substituents favor the retro-Prato cycloaddition by stabilizing the negative charge on the carbon atom of the azomethine ylide.

The energy profile for this process (**4b**→C_{60}+**6b**) is given in Figure 3, whereas Figure 4 depicts the molecular structure of the TS for this reaction. The imaginary frequency of this TS is 244.5i cm^{-1}. Not surprisingly, the asymmetry of the TS increases for the substituted species, with C−C bond lengths between the bonds being broken of 2.24 and 2.72 Å. As ex-

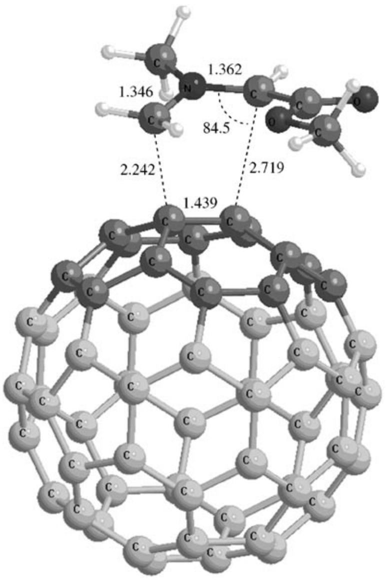

Figure 4. Optimized structure (ONIOM2(UB3LYP/6-31G(d):SVWN/STO-3G)) for **TS1b** with the most relevant bond lengths [Å] and angles [°]. H atoms and dark-grey atoms constitute the small system treated at a high level in the ONIOM approach.

pected from the steric hindrance, the largest C−C bond length occurs between the substituted C atom and the corresponding C atom of C_{60}. In this case, the intermediate formed by the interaction between the 1,3-dipole and the C_{60} cage is more stable because the dipole moment of the substituted azomethine ylide (4.660 D) is significantly larger than that of the unsubstituted 1,3-dipole (1.660 D). Despite the overall stabilization of the TS and the products, the reaction **4b**→**C_{60}+6b** is still quite endothermic and does not take place as found experimentally.[9] The energy profile clearly indicates that the equilibrium between reactants **4b** and products **C_{60}+6b** is totally displaced to the reactants side and possible products formed after severe heating will revert to reactants.

Retro-Prato cycloaddition assisted by maleic anhydride: Scheme 4 depicts the reaction mechanism studied in this section. Figure 5 contains the relative energies and Gibbs free energies of the TSs and products of the retrocycloaddition assisted by maleic anhydride. For the unsubstituted system (R^1=H), the energy barrier decreases by about 5 kcal mol^{-1} in the retrocycloaddition assisted by maleic anhydride. However, since entropy decreases when going from **4a+5** to **TS3a**, the Gibbs free energy barrier at 298 K increases by about the same quantity. Therefore, the presence of maleic anhydride does not improve the efficiency of the retrocycloaddition by reducing the barrier. Rather, the effect we find in this case is almost purely thermodynamic: the reaction now becomes exothermic by about 16 kcal mol^{-1} because of the increased stability of the final products. The energy profile depicted in Figure 5 clearly indicates that the equilibrium between reactants and products is now displaced to the products side and once the products are formed after heating they do not revert to reactants.

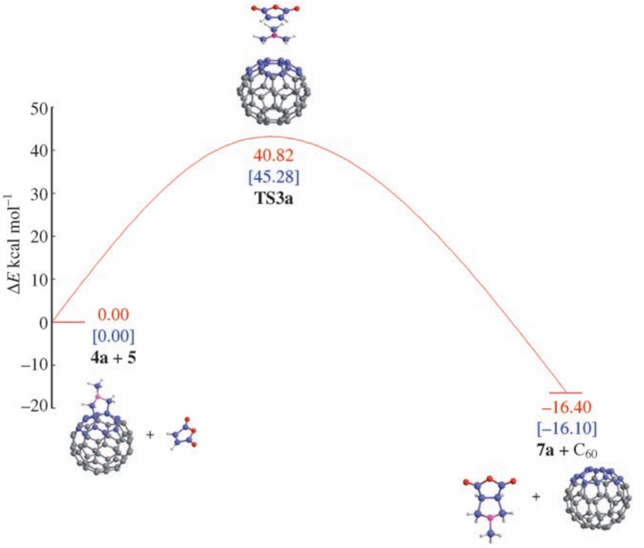

Figure 5. ONIOM2(UB3LYP/6-31G(d):SVWN/STO-3G) reaction energy profile (Gibbs free energies in square brackets) for the retrocycloaddition reaction assisted by maleic anhydride of the unsubstituted system.

Figure 6 shows that the TS structure for the *endo* approach of the retrocycloaddition assisted by maleic anhydride is slightly asymmetric. The totally symmetric TS that we have found is about 0.28 kcal mol^{-1} higher in energy than the slightly asymmetric TS.[20b] Moreover, the *endo* approach between the maleic anhydride and the ylide has been found to have a lower energy barrier, with a TS that is about 2.5 kcal mol^{-1} more stable than the *exo* TS. It is interesting to see how maleic anhydride provides assistance in this TS. The bond lengths between the C−C bonds connecting C_{60} and the azomethine ylide in the reactants are shorter than the new C−C bonds that are being formed between maleic anhydride and the azomethine ylide and, therefore, this TS has reactant-like character. The imaginary frequency of this TS is 179.2i cm^{-1}.

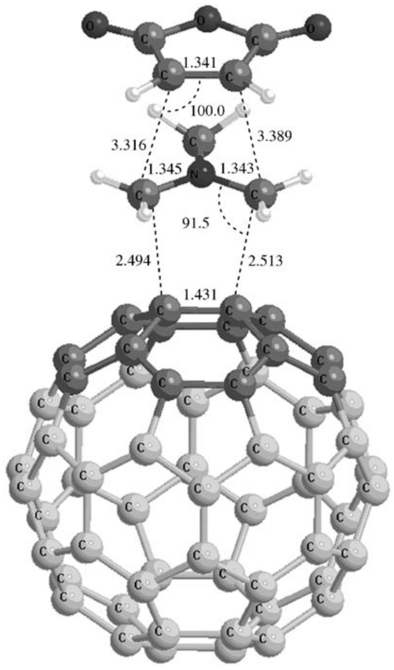

Figure 6. Optimized structure (ONIOM2(UB3LYP/6-31G(d):SVWN/STO-3G)) for **TS3a** with the most relevant bond lengths [Å] and angles [°]. H atoms and dark-grey atoms constitute the small system treated at high level in the ONIOM approach.

There is still another possible mechanism that can be operative for the retrocycloaddition assisted by maleic anhydride. In this case, the reaction would proceed from **4a** to C_{60}+**6a** and after that **6a** would react with maleic anhydride (**5**) to give the final nitrile oxide product **7a** (see Figure 2). Thus, in this case, the assistance of maleic anhydride does not occur along the whole reaction path, but only at the end of the reaction, just to stabilize the azomethine ylide formed. All attempts to find the TS of the reaction **6a+5**→**7a** have been unfruitful. Indeed, any optimization we have carried out by starting from any structure close to the final products (for instance by starting from C−C bond lengths of

4 Å) reverts to the final product **7a**. This indicates that the **6a**+**5**→**7a** conversion is an almost barrierless process, and that, in the presence of a dipolarophile, once **6a** is formed it is immediately transformed into **7a**. The whole energy barrier for **4a**+**5**→C_{60}+**7a** indicates that the process is assisted by the dipolarophile only at the end of the reaction (Figure 2) and is somewhat higher in energy than that of the retrocycloaddition assisted by maleic anhydride throughout the whole reaction (Figure 5). However, the free-energy profile for the latter is entropically unfavorable and, as a consequence, the free-energy profile at 298 K favors the mechanism in which the assistance of maleic anhydride does not occur along the whole reaction path, but only at the end of the reaction. Given the accuracy and reliability of the method employed for the calculation, we consider that it is not possible to rule out either of these two mechanisms for the retrocycloaddition assisted by maleic anhydride for the unsubstituted system (R^1=H), and that both mechanisms can be operative under intense heating of pyrrolidino[3,4:1,2,60]fullerenes in the presence of maleic anhydride.

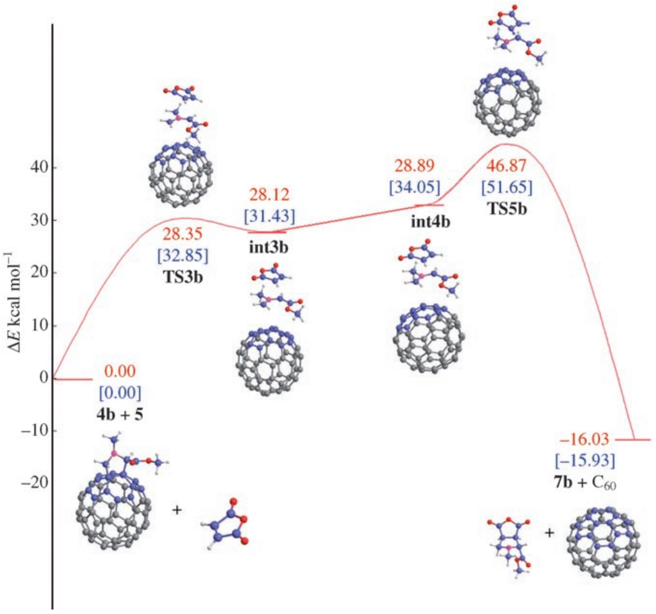

Figure 7. ONIOM2(UB3LYP/6-31G(d):SVWN/STO-3G) reaction energy profile (Gibbs free energies in square brackets) for the retrocycloaddition reaction assisted by maleic anhydride of the substituted system (R^1=$COOCH_3$).

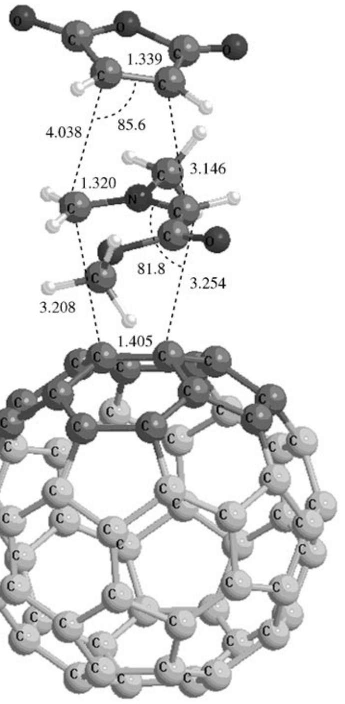

Figure 8. Optimized structure (ONIOM2(UB3LYP/6-31G(d):SVWN/STO-3G)) for **TS3b** with the most relevant bond lengths [Å] and angles [°]. H atoms ant dark-grey atoms constitute the small system treated at high level in the ONIOM approach.

We have also analyzed the retrocycloaddition assisted by maleic anhydride for the substituted system (R^1=$COOCH_3$). The energy profile with the relative energies and Gibbs free energies obtained for the process assisted by maleic anhydride along the reaction coordinate is given in Figure 7. The first TS has a lower energy barrier than the equivalent TS for the unassisted reaction, although the Gibbs free energy barriers are similar. The structure of this TS, which has an imaginary frequency of 16.8i cm^{-1}, is shown in Figure 8. This TS together with intermediates **int3b** and **int4b** reside on a relatively flat plateau. The presence of these intermediates, which were not found for the unsubstituted case, is favored by the higher dipole moment of the substituted azomethine ylide. In these intermediates, the C–C bonds that are being broken are not completely separated nor are the new C–C bonds totally formed. We have performed a linear transit of five steps from **int3b** to **int4b** by increasing/decreasing the four C–C bonds that are being broken or formed. The process has been carried out by using different uniform steps for each of the four coordinates. The coordinate value $R^i_{\text{linear transit}}$ at each step is given in Equation (1) as:

$$R^i_{\text{linear transit}} = R_{\mathbf{int3b}} + i\frac{(R_{\mathbf{int4b}} - R_{\mathbf{int3b}})}{6} \qquad (1)$$

in which, i=1 to 5 and $R_{\mathbf{int3b}}$ is the coordinate value for **int3b** and $R_{\mathbf{int4b}}$ is the coordinate value for **int4b**. The remaining geometrical parameters are then reoptimized. As a result we have obtained a linear transit with a continuous increase of energy from **int3b** to **int4b** as depicted in Figure 6. Therefore, we have not obtained an energy maximum from which to initiate the search for the TS that must exist between intermediates **int3b** and **int4b**. However, with this linear transit we have proven that this TS is probably quite close both in energy and structurally to **int4b**. The last TS corresponds to the formation and separation of the final nitrile oxide and pristine fullerene (**TS5b**). As compared to reactants, the energy of this TS is as high as 46.9 kcal mol^{-1} (Gibbs free energy of 51.7 kcal mol^{-1}) and, consequently, overall the mechanism of retrocycloaddition assisted by maleic anhydride for the substituted system along the reaction coordinate cannot compete with the mechanism of retrocycloaddition assisted by maleic anhydride only at the end of the reaction, that is, the reaction proceeds from **4b** to C_{60}+**6b** and after that **6b** reacts with maleic anhydride (**5**) to give the final product **7b**. The latter process has an overall energy barrier of only 32.9 kcal mol^{-1} (the free-energy value is 28.8 kcal mol^{-1}) as seen in Figure 3.

Finally, we have computed the thermodynamics of the retroreaction for the *N*-benzoyl pyrrolidinofullerenes with R = COPh, R^1 = COOMe and R^2 = H (Scheme 1). The energy needed to release the 1,3-dipole without the presence of dipolarophile in this system is 40.36 kcal mol^{-1}, that is, 1.6 kcal mol^{-1} higher than that found for **4b**. This result indicates that the benzoyl substituent destabilizes the azomethine ylide generated, thus impeding the reaction.

Conclusion

In summary, we have carried out new reactions on pyrrolidinofullerines with different substitution patterns on the C-2 and C-5 atoms of the pyrrolidine ring, which have a strong impact on the stability of the resulting azomethine ylides generated in the retrocycloaddition process. The nature of the substituent on the pyrrolidine nitrogen atom also has a great impact on the retrocyclization process. Thus, whereas methyl (or alkyl) and N−H groups undergo the retrocycloaddition quantitatively, the presence of a benzoyl group prevents or hinders this process.

In agreement with the experimental findings, theoretical calculations carried out at the DFT level and by using the two-layered ONIOM approach predict that the presence of the dienophile is not required for removal of the azomethine ylide from the fullerene surface which, after in-situ generation under thermal conditions, is trapped by the dipolarophile (maleic anhydride or *N*-phenylmaleimide). However, for the N-unsubstituted pyrrolidinofullerenes, it is possible that the dipolarophile can assist the 1,3-dipole to leave and, therefore, this alternative mechanism cannot be totally ruled out.

The results now reported on the scope and trapping experiments of the retrocycloaddition process of pyrrolidinofullerenes have allowed us to unravel the mechanism of this reaction, which has already been successfully used as a new and efficient protection–deprotection protocol in fullerene science, paves the way for further application of this reaction in the construction of new and fascinating fullerene-based carbon nanostructures.

Experimental Section

Computational details: Full geometry optimizations have been carried out with the two-layered ONIOM approach[22] by using the Gaussian 03 program.[23] The DFT X_α exchange (α = 2/3) functional[24a] in conjunction with the electron gas correlation functional (in Vosko–Wilk–Nusair parametrization)[24b], that is, the so-called SVWN method together with the standard STO-3G basis set[25] was used for the low level calculations and the hybrid density functional B3LYP method[26] with the standard 6-31G(d) basis set[27] was employed for the high level system. All systems were treated with the spin-restricted formalism. The choice of DFT methods was based on previous studies, which showed that DFT (and, in particular, the relatively inexpensive B3LYP method combined with the 6-31G(d) or similar basis set) provides a reliable description of reaction mechanisms of pericyclic reactions.[16,28] All stationary points found have been characterized as either minima or TSs by computing the vibrational harmonic frequencies; TSs have a single imaginary frequency with the corresponding eigenvector (transition vector) related to the approach of the two reaction centers, whereas minima have all real frequencies.

Gibbs-free-energy differences at 298.15 K and 1 atm. (ΔG_{298}) were calculated from electronic energies (ΔE) according to Equations 2 and 3, assuming an ideal gas:[29]

$$\Delta G_{298} = \Delta H_{298} - T\Delta S_{298} \tag{2}$$

with T = 298.15 K and

$$\Delta H_{298} = \Delta E + \Delta E^0_{\mathrm{vib}} + \Delta E^{298}_{\mathrm{trans}} + \Delta\, E^{298}_{\mathrm{rot}} + \Delta(\Delta E^0_{\mathrm{vib}})_{298} + \Delta(pV) \tag{3}$$

in which, $\Delta E^{298}_{\mathrm{trans}}$, $\Delta\, E^{298}_{\mathrm{rot}}$, and $\Delta E^0_{\mathrm{vib}}$ are the differences between products and reactants in translational, rotational and zero-point vibrational energy, respectively; $\Delta(\Delta E^0_{\mathrm{vib}})_{298}$ is the change in the vibrational energy difference as one goes from 0 to 298.15 K. The molar work term $\Delta(pV)$ is $(\Delta n)RT$ (e.g., for two fragments combining to give one molecule $\Delta n = -1$).

Acknowledgements

Financial help has been provided by the Spanish MEC (projects nos. CTQ2005–08797-C02–01/BQU, YCTQ2005–02609/BQU), the Consolider–Ingenio(2010C-07–25200), the CAM (project no. S-0505/PPQ/0225), and by the DURSI (project no. 2005SGR-00238). S.O. and S.F. thank the MEC for a research grant and for a Ramón y Cajal contract, respectively. We also acknowledge the Centre of Supercomputació of Catalunya (CESCA) for partial funding of computer time.

---

[1] a) H. W. Kroto, J. R. Heath, S. C. O'Brien, R. F. Curl, R. E. Smalley, *Nature* **1985**, *318*, 162–163; Nobel Lectures: b) R. E. Smalley, *Angew. Chem.* **1997**, *109*, 1666–1673; *Angew. Chem. Int. Ed. Engl.* **1997**, *36*, 1594–1601; c) H. W. Kroto, *Angew. Chem.* **1997**, *109*, 1648–1664; *Angew. Chem. Int. Ed. Engl.* **1997**, *36*, 1578–1593; d) R. F. Curl, *Angew. Chem.* **1997**, *109*, 1636–1647; *Angew. Chem. Int. Ed. Engl.* **1997**, *36*, 1566–1576.

[2] S. Iijima, *Nature* **1991**, *354*, 56–58.

[3] For a recent review, see: J. L. Delgado, M. A. Herranz, N. Martín, *J. Mater. Chem.* **2008**, *18*, 1417.

[4] For some recent books: a) A. Hirsch, *The Chemistry of Fullerenes*, Wiley-VCH, Weinheim (Germany), **2005**; b) *Fullerenes: From Synthesis to Optoelectronic Properties* (Eds.: D. M. Guldi, N. Martín), Kluwer Academic Publishers, Dordrecht (The Netherlands), **2002**; c) R. Taylor, *Lecture Notes on Fullerene Chemistry: A Handbook for Chemists*, Imperial College Press, London, **1999**; d) S. Reich, C. Thomsen, J. Maultzsch, *Carbon Nanotubes: Basic Concepts and Physical Properties*, Wiley-VCH, Weinheim (Germany), **2004**;

e) *Fullerenes*, (Eds.: F. Langa, J.-F. Nierengarten), RSC Publishing, Cambridge (UK), **2007**.

[5] a) N. Martín, *Chem. Commun.* **2006**, 2093–2104; b) N. Martín, M. Altable, S. Filippone, A. Martín-Domenech, *Synlett* **2007**, *20*, 3077–3095; c) special issue on *Functionalised Fullerene Materials, J. Mater. Chem.* **2002**, *12*, 1931–2159; d) special issue on the *Supramolecular Chemistry of Fullerenes Tetrahedron* **2006**, *9*, 1905–2132.

[6] a) N. Martín, M. Altable, S. Filippone, A. Martín-Domenech, *Chem. Commun.* **2004**, 1338–1339; b) N. Martín, M. Altable, S. Filippone, A. Martín-Domenech, A. Poater, M. Solà, *Chem. Eur. J.* **2005**, *11*, 2716–2729.

[7] N. Martín, M. Altable, S. Filippone, A. Martín-Domenech, M. Güell, M. Solà, *Angew. Chem.* **2006**, *118*, 1467–1470; *Angew. Chem. Int. Ed.* **2006**, *45*, 1439–1442.

[8] a) M. Altable, S. Filippone, A. Martín-Domenech, M. Güel, M. Solà, N. Martín, *Org. Lett.* **2006**, *8*, 5959–5962; b) M. Güell, M. Altable, S. Filippone, A. Martín-Domenech, N. Martín, M. Solà, *J. Phys. Chem. A* **2007**, *111*, 5253–5258.

[9] N. Martín, M. Altable, S. Filippone, A. Martín-Domenech, L. Echegoyen, C. M. Cardona, *Angew. Chem.* **2006**, *118*, 116–120; *Angew. Chem. Int. Ed.* **2006**, *45*, 110–114.

[10] a) M. Maggini, G. Scorrano, M. Prato, *J. Am. Chem. Soc.* **1993**, *115*, 9798–9799; b) N. Tagmatarchis, M. Prato, *Synlett* **2003**, 768–779.

[11] N. Martín, J. L. Segura, F. Wudl in *Fullerenes: From Synthesis to Optoelectronic Properties* (Eds.: D. M. Guldi, N. Martín), Kluwer Academic Publishers Dordrecht (The Netherlands), **2002**, Chapter 3, pp. 81–120.

[12] a) C. Bingel, *Chem. Ber.* **1993**, *126*, 1957–1959; b) X. Camps, A. Hirsch, *J. Chem. Soc. Perkin Trans. 1* **1997**, 1595–1596.

[13] a) M. Prato, M. Maggini, *Acc. Chem. Res.* **1998**, *31*, 519–526; b) M. Maggini, E. Menna, in *Fullerenes: From Synthesis to Optoelectronic Properties* (Eds.: D. M. Guldi, N. Martín), Kluwer Academic Publishers, Dordrecht (The Netherlands), **2002**, Chapter 1, pp. 1–50.

[14] O. Lukoyanova, C. M. Cardona, M. Altable, S. Filippone, A. Martín-Domenech, N. Martín, L. Echegoyen, *Angew. Chem.* **2006**, *118*, 7590–7593; *Angew. Chem. Int. Ed.* **2006**, *45*, 7430–7433.

[15] E. Vedejs, J. W. Grissom *J. Am. Chem. Soc.* **1988**, *110*, 3238–3246.

[16] M. Cases, M. Duran, J. Mestres, N. Martín, M. Solà, *J. Org. Chem.* **2001**, *66*, 433–442.

[17] a) M. Cases, M. Duran, J. Mestres, N. Martín, M. Solà in *Fullerenes for the New Millennium* (Eds.: P. V. Kamat, K. M. Kadish, D. M. Guldi), *Vol. 11*, The Electrochemical Society, Pennington, **2001**, pp. 244–269; b) E. U. Wallenborn, R. F. Haldimann, F. G. Klarner, F. Diederich, *Chem. Eur. J.* **1998**, *4*, 2258–2265; c) X. Zhuang, Z. Yang, J. Zhang, W. Cao, *J. Mol. Struct. (Theochem)* **2006**, *760*, 45–52.

[18] Z. Shang, Y. Pan, Z. Cai, X. Zhao, A. Tang, *J. Phys. Chem. A* **2000**, *104*, 1915–1919.

[19] L. Türker, *J. Mol. Struct. (Theochem)* **2002**, *588*, 165–174.

[20] a) We have been unable to reach full convergence for this transition state because of the extreme flatness of the surface around this position. The root-mean-square value for the forces converged and the maximum force at this point was less than 1×10^{-3} a.u. However, the displacements did not fully converge. b) The lack of symmetry in this TS is not totally unexpected, see: S. M. Bachrach, P. B. White, *J. Mol. Struct (Theochem)* **2007**, *819*, 72–78.

[21] C. Hansch, A. Leo, R. W. Taft, *Chem. Rev.* **1991**, *91*, 165–195.

[22] a) M. Svensson, S. Humbel, R. D. J. Froese, T. Matsubara, S. Sieber, K. Morokuma, *J. Phys. Chem.* **1996**, *100*, 19357–19363; b) S. Dapprich, I. Komáromi, K. S. Byu, K. Morokuma, M. J. Frisch, *J. Mol. Struct. (Theochem)* **1999**, *461–462*, 1–21.

[23] Gaussian 03, Revision C.01 ed., M. J. Frisch, G. W. Trucks, H. B. Schlegel, G. E. Scuseria, M. A. Robb, J. R. Cheeseman, J. A. Montgomery Jr., T. Vreven, K. N. Kudin, J. C. Burant, J. M. Millam, S. S. Iyengar, J. Tomasi, V. Barone, B. Mennucci, M. Cossi, G. Scalmani, N. Rega, G. A. Petersson, H. Nakatsuji, M. Hada, M. Ehara, K. Toyota, R. Fukuda, J. Hasegawa, M. Ishida, T. Nakajima, Y. Honda, O. Kitao, H. Nakai, M. Klene, X. Li, J. E. Knox, H. P. Hratchian, J. B. Cross, V. Bakken, C. Adamo, J. Jaramillo, R. Gomperts, R. E. Stratmann, O. Yazyev, A. J. Austin, R. Cammi, C. Pomelli, J. W. Ochterski, P. Y. Ayala, K. Morokuma, G. A. Voth, P. Salvador, J. J. Dannenberg, G. Zakrzewski, S. Dapprich, A. D. Daniels, M. C. Strain, O. Farkas, D. K. Malick, A. D. Rabuck, K. Raghavachari, J. B. Foresman, J. V. Ortiz, Q. Cui, A. G. Baboul, S. Clifford, J. Cioslowski, B. B. Stefanov, G. Liu, A. Liashenko, P. Piskorz, I. Komaromi, R. L. Martin, D. J. Fox, T. Keith, M. A. Al-Laham, C. Y. Peng, A. Nanayakkara, M. Challacombe, P. M. W. Gill, B. Johnson, W. Chen, M. W. Wong, C. Gonzalez, J. A. Pople, Gaussian, Inc. Pittsburgh, PA, **2003**.

[24] a) J. C. Slater, *Quantum Theory of Molecules and Solids, Vol. 4*, McGraw-Hill, New York, **1974**; b) S. H. Vosko, L. Wilk, M. Nusair, *Can. J. Phys.* **1980**, *58*, 1200–1211.

[25] W. J. Hehre, R. F. Stewart, J. A. Pople, *J. Chem. Phys.* **1969**, *51*, 2657–2664.

[26] a) A. D. Becke, *J. Chem. Phys.* **1993**, *98*, 5648–5652; b) C. Lee, W. Yang, R. G. Parr, *Phys. Rev. B* **1988**, *37*, 785–789; c) P. J. Stephens, F. J. Devlin, C. F. Chabalowski, M. J. Frisch, *J. Phys. Chem.* **1994**, *98*, 11623–11627.

[27] a) W. J. Hehre, R. Ditchfield, J. A. Pople, *J. Chem. Phys.* **1972**, *56*, 2257–2261; b) P. C. Hariharan, J. A. Pople, *Theor. Chim. Acta* **1973**, *28*, 213–222.

[28] a) M. Freccero, R. Gandolfi, M. Sarziamade, A. Rastelli, *J. Chem. Soc. Perkin Trans. 2* **1998**, 2413–2419; b) O. Wiest, K. N. Houk, K. A. Black, B. Thomas, *J. Am. Chem. Soc.* **1995**, *117*, 8594–8599; c) O. Wiest, K. N. Houk, *Top. Curr. Chem.* **1996**, *183*, 1–24; d) E. Goldstein, B. Beno, K. N. Houk, *J. Am. Chem. Soc.* **1996**, *118*, 6036–6043; e) T. C. Dinadayalane, R. Vijaya, A. Smitha, G. N. Sastry, *J. Phys. Chem. A* **2002**, *106*, 1627–1633; f) H. Isobe, S. Yamanaka, K. Yamaguchi, *Int. J. Quantum Chem.* **2003**, *95*, 532–545; g) C. Di Valentin, M. Freccero, R. Gandolfi, A. Rastelli, *J. Org. Chem.* **2000**, *65*, 6112–6120.

[29] P. W. Atkins, *Physical Chemistry*, Oxford University Press, Oxford, **1982**.

Received: January 17, 2008